(1) The application of conventional tunneling hopping theories,[16] in order to explain the large jump rate at 1 K in pure Al, results in unrealistically large values of J.

(2) The very small activation energy derived from the τ_c data above 20 K rules out the trapping at impurities below 20 K.

(3) The relation between the strain-induced energy shift ΔE and the tunneling matrix element J of the muon fulfills consistently the requirements of the Anderson theory.[18] For the case of pure Al we find $J \gg \Delta E$.

The above interpretation is also supported by the fact that the EFG at the Al is characteristic for an interstitial muon acting on the Al rather than for a neighboring Mn atom. The absolute value of the EFG derived from the same data is close to the theoretical prediction given for pure Al metal.[14] The strain-induced self-trapping mechanism in Al is supposed to occur even at much lower concentrations of Mn than used here. In order to observe the transition between both regimes, experiments with lower Mn content are under way.

We thank K. W. Kehr, L. Pernestål, and J. C. Soulié for helpful discussions, and J. J. Fenzl for the preparation of the sample.

[1]V. G. Grebinnik *et al.*, Zh. Eksp. Teor. Fiz. 68, 1548 (1975) [Sov. Phys. JETP 41, 777 (1976)].
[2]O. Hartmann *et al.*, Phys. Lett. 61A, 141 (1977).
[3]O. Hartmann *et al.*, Hyperfine Interact. 4, 824 (1978).
[4]A. T. Fiory *et al.*, Phys. Rev. Lett. 40, 968 (1978)
[5]R. H. Heffner *et al.*, Hyperfine Interact. 4, 838 (1978).
[6]V. G. Grebinnik *et al.*, Pis'ma Zh. Eksp. Teor. Fiz. 25, 322 (1977) [JETP Lett. 25, 298 (1977)].
[7]M. Borghini *et al.*, Phys. Rev. Lett. 40, 1723 (1978).
[8]H. K. Birnbaum *et al.*, Phys. Lett. 65A, 435 (1978).
[9]W. Schmatz, *Treatise of Materials Science and Technology*, edited by H. Hermans (Academic, New York, 1973), Vol. 2.
[10]G. S. Bauer, Institut für Festkörperforschung der Kernforschungsanlage Jülich Report No. JÜL-1158, 1975 (unpublished).
[11]O. Hartmann, Phys. Rev. Lett. 39, 832 (1977).
[12]J. P. Bugeat *et al.*, Phys. Lett. 58A, 127 (1976).
[13]N. Kroó and U. Szentivmay, Phys. Rev. B 10, 278 (1974).
[14]P. Jena *et al.*, Phys. Rev. Lett. 40, 264 (1978).
[15]C. Berthier and M. Minier, J. Phys. F 7, 515 (1977).
[16]C. P. Flynn and A. M. Stoneham, Phys. Rev. B 1, 3966 (1970).
[17]Y. Kagan and M. I. Klinger, J. Phys. C 7, 2791 (1974).
[18]P. W. Anderson, Phys. Rev. 109, 1492 (1958).
[19]G. Leibfried, Z. Phys. 135, 23 (1953).
[20]B. Baranowski *et al.*, J. Phys. F 1, 258 (1971).

Origin of Thermal Conductivity Anisotropy in Liquid Crystalline Phases

F. Rondelez, W. Urbach, and H. Hervet
Collège de France, Physique de la Matière Condensée, Paris Cedex 75231, France
(Received 12 April 1978)

Thermal conductivity measurements have been performed in nematic and smectic liquid crystalline phases by the forced Rayleigh light-scattering technique. Results show clearly that the thermal transport anisotropy is governed by the molecular shape anisotropy and by the molecular orientation but is independent of the smectic layer ordering.

Most of the past work on thermal transport has been devoted to thermal conductivity measurements in nematic phases. Despite some initial controversies, it is now accepted that the conductivity is anisotropic, being maximum (minimum) parallel (perpendicular) to the direction of the local optical axis.[1] Recently we have been able to extend the measurement down into the smectic-A phases. The preliminary results have indicated that thermal transport properties are not influenced by the regular layered structure.[2] This behavior is rather unexpected since it has been demonstrated that the smectic layers act as strong barriers to molecular motion in other transport properties as mass diffusion and ionic conductivity.[3]

In this Letter, we clearly ascertain that heat transport is primarily governed by the individual molecular properties and the orientational ordering but not by the long-range position ordering. Thermal conductivity data are presented on nematic compounds with different molecular lengths, in an attempt to vary the molecular geometrical shape anisotropy. The angular dependence of the thermal diffusivity is also investigated on both sides of a smectic-C to nematic phase transition.

The smectic-C phase is interesting since the molecular orientation no longer coincides with the normal to the smectic layers as in the smectic-A phase.

Thermal diffusivity measurements have been performed by the forced Rayleigh light-scattering technique[4] with an experimental setup identical to that of Ref. 2. The temperature fluctuations are generated artificially by illuminating the liquid crystal sample with an optical fringe pattern obtained by interfering two light beams from the same laser. If the sample is absorbing at the laser wavelength, a temperature grating will be set up which in turn will modulate the refractive index. The thermal pattern thus gives rise to an optical phase diffraction grating which is probed by a separate low-power laser. When the light fringe pattern is switched off, the diffraction grating decays exponentially with a single time constant $\tau = 1/Dq^2$, where D is the thermal diffusivity to be measured and q is the grating wave vector. There are no further complications such as coupling between the thermal relaxation process by thermal diffusivity and the long-wavelength nematic director fluctuations. Truly, the local temperature changes modify the magnitude of the nematic order parameter S.[5] However, since S does not obey a conservation law, it always adjusts to the local temperature distribution in microscopic times.[6] The long-lived modes of the director fluctuations, which have characteristic frequencies[7] η/Kq^2 comparable to τ^{-1}, are not affected (K is an elastic constant, η a viscosity coefficient). This is evidenced experimentally by the absence of any strong depolarized component in the diffracted light intensity.

Several liquid crystals, with various mesomorphic phases, have been investigated. Their chemical formulas and phase diagrams are presented in Table I. The liquid-crystal samples were placed between two SiO-coated glass plates separated by 150-μm spacers. With the plates properly coated and oriented,[8] uniaxial alignment of the nematic phases is achieved with the molecules parallel to the glass walls. However, when cooling down into the smectic-C phase of DOBCP and OAB, stabilizing high-frequency electric fields ($4\times 10^2 V_{rms}$, 10 kHz) were also applied on the sample to prevent the molecules from rotating out of the plane of the glass plates. With tangential boundary conditions for the molecules, large focal conics (~ 2 m/m^2) are formed.[5] The ellipses are generally stuck to the glass walls. They have two main orientations, either parallel to the easy alignment axis or at a well-defined, finite angle to it. This angle is observed to correspond to the tilt angle $\theta_{tilt} \simeq 32°$ for OAB[9] and $\simeq 45°$ for DOBCP.[10] A similar situation has already been reported by

TABLE I. K-15 denotes 4′-n-pentyl-4-cyanobiphenyl, T-15 denotes 4′-n-pentyl-4-cyanoterphenyl, OAB denotes 4,4′-di-n-octyloxy azoxy benzene, DOBCP denotes di-(4-n-decyloxybenzal)-2-chloro-1-4-phenylene diamine.

(K-15) C_5H_{11}–⟨⟩–⟨⟩–CN

solid —22.5°C→ nematic —35°C→ isotropic liquid

(T-15) C_5H_{11}–⟨⟩–⟨⟩–⟨⟩–CN

solid —131°C→ nematic —239°C→ isotropic liquid

(OAB) $H_{17}C_8O$–⟨⟩–N(O)=N–⟨⟩–OC_8H_{17}

solid —80°C→ smectic C —108°C→ nematic —126°C→ isotropic liquid

(DOBCP) $H_{21}C_{10}O$–⟨⟩–CH=N–⟨Cl⟩–N=CH–⟨⟩–$OC_{10}H_{21}$

solid —66°C→ smectic C —112.5°C→ nematic —166.5°C→ isotropic liquid

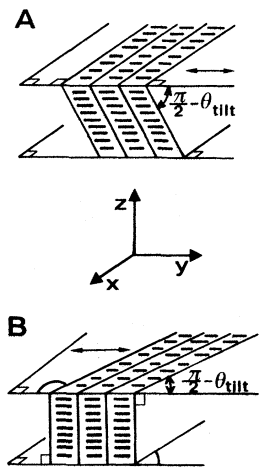

FIG. 1. Schematic representation of the two smectic layers orientations relative to the glass boundaries and to the easy alignment axis observed in the smectic-C phase of 4,4′-di-n-octyloxy azoxy benzene and of di-(4-n-decyloxybenzal)-2-chloro-1-4-phenylene diamine. The easy alignment axis, defined by the skewed evaporation conditions, is represented by the double arrow parallel to Oy. The sharply defined smective planes have no real physical meaning and are just a guide to the eye.

Lefèvre *et al.*[11] The two types of domains correspond to two different orientations of the smectic planes relative to the glass walls (see Fig. 1). In domains A, the planes are at a finite angle from the normal to the walls (Oz) and cross the glass planes (xOy) perpendicularly to the easy alignment axis (Oy). In domains B, the planes are parallel to Oz and cross the xOy planes at $\frac{1}{2}\pi - \theta_{\text{tilt}}$ to Oy. This latter geometry is the simplest for anisotropic thermal diffusivity measurements and will always be chosen experimentally. The angular dependence of D is obtained by rotating the fringe pattern (generally formed of regularly spaced stripes) relative to the principal axes of the oriented samples. D is then the thermal diffusivity perpendicular to the stripes.

Results are first given for the nematic phases. Figure 2 shows the dependence of the decay time τ of the thermal phase grating versus the inverse square of the grating wave vector q for T-15 and K-15. The fringe spacing has been varied between 20 and 60 μm, always well below the sample thickness to avoid edge effects.[2] For each compound, two sets of measurements have been performed to measure the thermal diffusivity coefficients parallel ($D_{\parallel}$) and perpendicular ($D_{\perp}$) to the average orientation of the long molecular axis. As expected for a purely diffusing process, the curves are linear and $\tau = (Dq^2)^{-1}$. From the slopes we get $D_{\parallel} = (1.25 \pm 0.05) \times 10^{-3}$ cm^2 sec^{-1} and $D_{\perp} = (0.79 \pm 0.04) \times 10^{-3}$ cm^2 sec^{-1} for K-15 at 25°C, $D_{\parallel} = (1.37 \pm 0.04) \times 10^{-3}$ cm^2 sec^{-1} and $D_{\perp} = (0.59 \pm 0.02) \times 10^{-3}$ cm^2 sec^{-1} for T-15 at 163°C. Separate measurements for OAB C give $D_{\parallel} = (12.4 \pm 0.10) \times 10^{-4}$ cm^2 sec^{-1} and $D_{\perp} = (4.7 \pm 0.10) \times 10^{-4}$ cm^2 sec^{-1} at 109°C.

The temperature dependence of $D_{\parallel}$ and $D_{\perp}$ in the nematic phase and of D_0 for the isotropic phase has also been measured. The results are quite similar to those already reported for other nematic materials.[1,2]

In the smectic-C phases, we are interested in

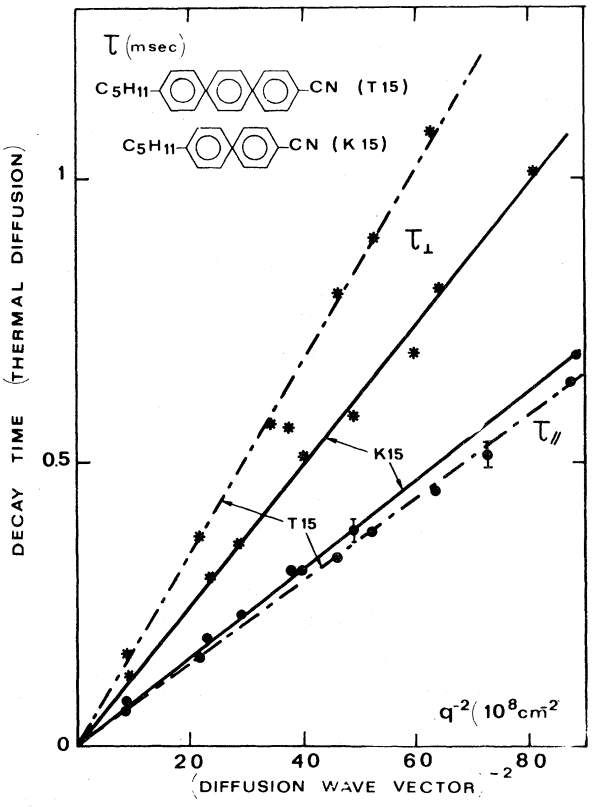

FIG. 2. Decay time of the laser-induced thermal grating vs the inverse square of the grating wave vector. (K-15) 4′-n-pentyl-4-cyanobiphenyl/nematic phase $T = 25$°C and (T-15) 4′-n-4-cyanoterphenyl/nematic phase $T = 163$°C.

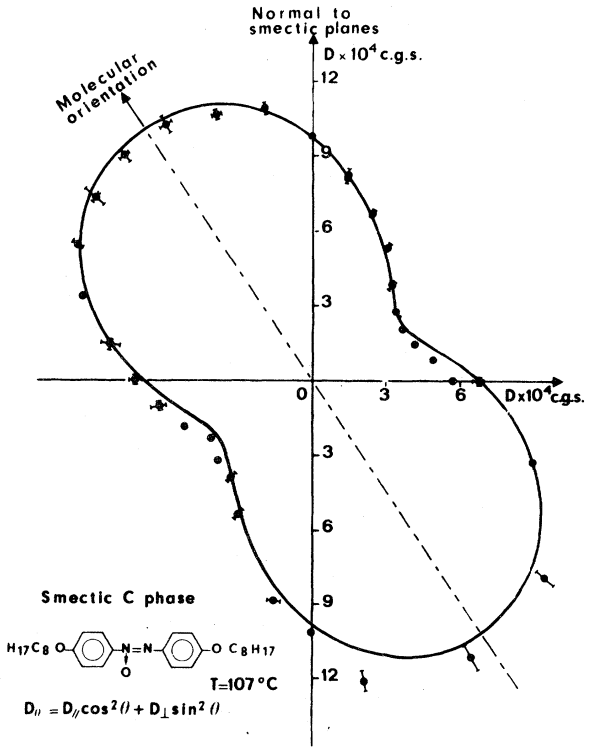

FIG. 3. Angular dependence of the thermal diffusivity coefficient with respect to the direction of the average molecular orientation and of the smectic layers normal. smectic-C phase of 4,4′-di-n-octyloxy azoxy benzene. $T = 107$°C. $D_{\parallel} = 12.2 \times 10^{-4}$ cm^2 sec^{-1}. $D_{\perp} = 4.4 \times 10^{-4}$ cm^2 sec^{-1}.

relating the thermal diffusivity anisotropy to the molecular orientation and to the direction of the smectic layers. We have performed the angular analysis of the thermal diffusivity in OAB and DOBCP. The results are shown on Fig. 3 for OAB. The polar plot of D vs θ has a characteristic "peanut shape," and the data points are well fitted by the equation $D(\theta) = D_{\parallel}\cos^2\theta + D_{\perp}\sin^2\theta$. One obtains $D_{\parallel} = (12.2 \pm 0.10) \times 10^{-4}$ cm^2 sec^{-1} and $D_{\perp} = (4.4 \pm 0.10) \times 10^{-4}$ cm^2 sec^{-1} for OAB at 107°C. For DOBCP a similar analysis yields $D_{\parallel} = (24.8 \pm 0.09) \times 10^{-4}$ cm^2 sec^{-1} and $D_{\perp} = (7.8 \pm 0.07) \times 10^{-4}$ cm^2 sec^{-1} at 111°C. In both cases one notices that (1) the polar diagram is peaked in the direction of the molecular orientation in the very same manner as for the nematic phase, and (2) the absolute D values are very close on both sides of the smectic-C to nematic phase transition.

Our present experiments raise an interesting question on the origin of the thermal conductivity anisotropy. It is obvious from all earlier results[1,2] that the anisotropy is dependent on the *orientational* degree of alignment. Actually, when the molecular orientation is at random, as in the isotropic phase, the thermal anisotropy falls to zero. Also the temperature dependence of $D_{\parallel}$ in the nematic phase follows the variation of the order parameter S.[5] On the other hand, our data on smectic-A,[2] smectic-B,[2] and smectic-C phases show that the long-range *positional* ordering of the centers of gravity of the molecules is not important to explain the thermal transport. At this stage one should then look at the molecular scale. Since the molecules are elongated, the simplest idea is to relate the thermal anisotropy to the geometrical shape anisotropy. This is indeed supported by the present experiments. Increasing the molecular length by one benzene ring between K-15 and T-15 increases the $D_{\parallel}/D_{\perp}$ ratio from 1.58 to 2.32. Also, comparing the $D_{\parallel}/D_{\perp}$ value obtained for OAB with the literature value of its lower homolog, the well-known p-azoxy anisol,[1] we get an increase from 1.5 to 2.7 for aliphatic end chains with one and eight carbon atoms, respectively. Last, very high anisotropic ratios $\simeq 3.2$ are obtained with strongly elongated moleculates such as DOBCP. These are by far the highest reported to date.

It is tempting to make the analogy between the isolated elongated molecules of the liquid crystalline compounds and the individual grains of polycrystalline solids. In these materials, the thermal conductivity depends on the grain dimensions because the mean free path of the thermal phonons is limited by the grain size. This is especially true at helium temperatures when the intrinsic mean free path, as measured in a perfect crystal, becomes very long.[12] In the liquid-crystal case, the molecules can be roughly considered as rigid rods of length $\simeq 20$ Å and width $\simeq 5$ Å. Literature data[13] quote the mean free path of the phononlike modes responsible for heat conduction in liquids in this very same range. Thus the above inequality condition is satisfied in liquids even near room temperature. It is then expected that the molecular dimensions will limit the phonon mean free path and consequently the thermal conductivity. Furthermore, if the molecular shape is anisotropic, the thermal conductivity will also be anisotropic.

In conclusion, measurements of the thermal diffusivity coefficients are reported in smectic-C phases for the first time. There is no peculiarity in the angular plots in the direction of the normal to the layers. This gives strong evidence that the thermal transport is not dependent on the long-range smectic layer ordering. Another important result is that the long-range orientational ordering merely helps to reveal more local anisotropic properties. We believe that the geometrical shape anisotropy of the molecules is the decisive factor in explaining the thermal transport anisotropy. Thus any future thermal transport theory in liquid crystalline phases should be made at the molecular level.

It is a pleasure to thank G. W. Gray for the generous supply of terphenyl in the early stages of this work. DOBCP and OAB have been kindly synthesized for us by L. Liebert and P. Keller at the Laboratoire de Physique des Solides–Orsay.

[1]R. Vilanove, E. Guyon, C. Mitescu, and P. Pieranski, J. Phys. (Paris) 35, 153 (1974).

[2]W. Urbach, H. Hervet, and F. Rondelez, to be published.

[3]A. Mircea-Roussel, L. Léger, F. Rondelez, and W. H. de Jeu, J. Phys. (Paris) 36, C1-93 (1975).

[4]H. Eichler, G. Salje, and H. Stahl, J. Appl. Phys. 44, 5383 (1973); D. W. Pohl, S. E. Schwarz, and V. Irniger, Phys. Rev. Lett. 31, 32 (1973).

[5]P. G. de Gennes, *The Physics of Liquid Crystals* (Clarendon, Oxford, 1974).

[6]P. C. Martin, O. Parodi, and P. S. Pershan, Phys. Rev. A 6, 2401 (1972).

[7]Orsay Group on Liquid Crystals, Mol. Cryst. Liq. Cryst. 13, 187 (1971).

[8]J. L. Janning, Appl. Phys. Lett. 21, 173 (1973).

[9]I. G. Chistyakov and W. M. Chaikowsky, Mol. Cryst.

Liq. Cryst. 7, 269 (1969).
[10]T. R. Taylor, J. L. Fergason, and S. L. Arora, Phys. Rev. Lett. 24, 359 (1970).
[11]M. Lefèvre, J. L. Martinand, G. Durand, and M. Veyassié, C. R. Acad. Sci., Ser. B 273, 403 (1971).
[12]See, e.g., P. G. Klemens, in *Solid State Physics*, edited by H. Ehrenreich, F. Seitz, and D. Turnbull (Academic, New York, 1958), Vol. 7, p. 1. (1958).
[13]P. A. Egelstaff, *An Introduction to the Liquid State* (Academic, New York, 1967).

Energy-Minimization Approach to the Atomic Geometry of Semiconductor Surfaces

D. J. Chadi
Xerox Palo Alto Research Center, Palo Alto, California 94304
(Received 13 June 1978)

The (110) surface atomic geometries of GaAs and ZnSe and of 2×1 reconstructed (111) surface of Si are calculated by minimizing the total energy of the electron-ion system. The corresponding reductions in total energy between the relaxed and unrelaxed surfaces are calculated to be −0.51, −0.30, and −0.37 eV per surface atom, respectively. Subsurface relaxations are generally found to make a very small (≤ 0.02 eV) contribution to the reduction in total energy.

Recent analyses of low-energy electron-diffraction (LEED) intensities have shown that atomic rearrangements on semiconductor surfaces are pervasive and involve large atomic displacements[1]. Additional evidence for this has come from studies of surface electronic structure. The metallic or nonmetallic nature of the surface, the positions of surface states, and their dispersion and symmetry are strongly dependent on the surface atomic geometry. In this way from a comparison of theoretical and experimental surface spectra information on surface structure has been obtained.[2-7]

In this Letter a total-energy-minimization approach to semiconductor surface-structure determination is presented. The only input into the calculation are from bulk electronic and lattice-dynamical properties. The approach is based on a semiempirical model for the variation of the total energy $\Delta E_{\rm tot}$ with changes in atomic coordinates. In the bulk, the elastic coefficients and phonons frequencies can be directly related to the variation in $E_{\rm tot}$ with atomic displacements; therefore, the accuracy of the model for $\Delta E_{\rm tot}$ can be easily tested. An energy-minimization approach to structural properties of crystals[8-10] and surfaces[11-15] has also been utilized in several recent works.

The total energy $E_{\rm tot}$ of an electron-ion system can be expressed as

$$E_{\rm tot} = E_{ee} + E_{ei} + E_{ii}, \tag{1}$$

where E_{ee}, E_{ei}, and E_{ii} denote the electron-electron, electron-ion, and ion-ion interaction energies, respectively. It is useful to introduce the "band-structure" energy defined as

$$E_{\rm bs} = \sum_{\vec{k},n} E_n(\vec{k}), \tag{2}$$

where the sum of single-particle energies is taken over occupied states, with wave vector $\vec{k}$ and band index n. In terms of $E_{\rm bs}$ and making use of the fact that $E_{\rm bs} = E_{ei} + 2E_{ee}$, Eq. (1) can be expressed as

$$E_{\rm tot} = E_{\rm bs} + U, \tag{3}$$

where $U = E_{ii} - E_{ee}$. The advantage of Eq. (3) over Eq. (1) is that for two ions that are separated by a distance much larger than the Thomas-Fermi screening length the combined ion-plus-screening-electron system is nearly neutral and U is close to zero. One would therefore expect that to a good approximation this term can be described by a short-range-force-constant model.

To calculate $E_{\rm bs}$ the Slater-Koster[16] tight-binding method was used. The tight-binding parameters were chosen to be identical to those used in our previous work[8] on structural properties of crystalline semiconductors. For the bulk the conditions imposed on $E_{\rm tot}$ were that at equilibrium it satisfy

$$\partial E_{\rm tot}/\partial V = 0 \tag{4}$$

and

$$V\partial^2 E_{\rm tot}/\partial V^2 = B, \tag{5}$$

where V denotes volume and B the bulk modulus. For a given dependence of the tight-binding param-

